Numerical study of discrete models in the class of the nonlinear molecular beam epitaxy equation

F. D. A. Aarão Reis
Instituto de Física, Universidade Federal Fluminense, Avenida Litorânea s/n, 24210-340 Niterói RJ, Brazil
(Received 15 March 2004; published 27 September 2004)

We study numerically some discrete growth models belonging to the class of the nonlinear molecular beam epitaxy equation, or the Villain–Lai–Das Sarma (VLDS) equation. The conserved restricted solid-on-solid model (CRSOS) with maximum height differences $\Delta H_{\max}=1$ and $\Delta H_{\max}=2$ was analyzed in substrate dimensions $d=1$ and $d=2$. The Das Sarma and Tamborenea (DT) model and a competitive model involving random deposition and CRSOS deposition were studied in $d=1$. For the CRSOS model with $\Delta H_{\max}=1$, we obtain the more accurate estimates of scaling exponents in $d=1$: roughness exponent $\alpha=0.94\pm0.02$ and dynamical exponent $z=2.88\pm0.04$. These estimates are significantly below the values of one-loop renormalization for the VLDS theory, which confirms Janssen's proposal of the existence of higher-order corrections. The roughness exponent in $d=2$ is very near the one-loop result $\alpha=\frac{2}{3}$, in agreement with previous works. The moments W_n of orders $n=2$, 3, 4 of the height distribution were calculated for all models, and the skewness $S\equiv W_3/W_2^{3/2}$ and the kurtosis $Q\equiv W_4/W_2^2-3$ were estimated. At the steady states, the CRSOS models and the competitive model have nearly the same values of S and Q in $d=1$, which suggests that these amplitude ratios are universal in the VLDS class. The estimates for the DT model are different, possibly due to their typically long crossover to asymptotic values. Results for the CRSOS models in $d=2$ also suggest that those quantities are universal.

DOI: 10.1103/PhysRevE.70.031607 PACS number(s): 81.15.Aa, 05.40.−a, 05.50.+q

I. INTRODUCTION

Surface and interface growth processes are subjects of great interest from the perspective of applications to thin films and multilayer growth, and, from the theoretical point of view, for their important role in nonequilibrium statistical mechanics [1,2]. Frequently, those processes are described by discrete models which represent the basic growth mechanisms by simple stochastic rules, such as aggregation and diffusion, and neglect details of the microscopic interactions. On the other hand, continuous theories are successful at representing those processes in the hydrodynamic limit. They predict the scaling exponents of many discrete models, which are consequently grouped in a small number of universality classes.

Growth by molecular beam epitaxy (MBE), which is one of the most important techniques to produce high-quality films with smooth surfaces, motivated the proposal of many discrete and continuous models. The dynamics during MBE deposition is dominated by diffusion processes, which led to the proposal of the Villain–Lai–Das Sarma (VLDS) growth equation [3,4]

$$\frac{\partial h}{\partial t} = \nu_4 \nabla^4 h + \lambda_4 \nabla^2 (\nabla h)^2 + \eta(\vec{x},t), \tag{1}$$

where $h(\vec{x},t)$ is the height at position $\vec{x}$ and time t in a d-dimensional substrate, ν_4 and λ_4 are constants, and η is a Gaussian (nonconservative) noise. Equation (1) is also frequently called a nonlinear molecular beam epitaxy equation or a conserved Kardar-Parisi-Zhang equation [1,5].

The most important geometrical quantity to characterize the surface of the deposit grown by such processes is the interface width. It is defined as the root-mean-square fluctuation of the average height,

$$\xi \equiv [\langle (h-\overline{h})^2 \rangle]^{1/2}. \tag{2}$$

For short times, it scales as

$$\xi \sim t^{\beta}, \tag{3}$$

where β is called the growth exponent. For long times, in the steady state, the interface width saturates at

$$\xi_{\text{sat}} \sim L^{\alpha}, \tag{4}$$

where α is called the roughness exponent. The crossover time from the growth regime to the steady state scales with L with the dynamical exponent

$$z = \alpha/\beta. \tag{5}$$

For the VLDS theory, a one-loop dynamical renormalization-group (DRG) calculation [3,4] led to $\alpha=(4-d)/3$, $z=(8+d)/3$, and $\beta=(4-d)/(8+d)$ below the upper critical dimension $d_c=4$. See also the recent work of Katzav [6], based on a self-consistent expansion approach, which also obtains these estimates. Some authors assumed the one-loop values to be exact in all orders, but Janssen [7] recently claimed that this conclusion was derived from an ill-defined transformation and, consequently, there would be higher-order corrections. From a two-loop calculation, he obtained small negative corrections to α and z in all dimensions [7]. Numerical studies of some discrete models which belong to the VLDS class in the continuum limit (large lattices, long times) were not able to solve this controversy. In $d=1$, numerical work on a conserved restricted solid-on-solid model (to be defined below) systematically suggests $\alpha<1$ [8,9], but the error bars are large and, consequently, the authors still suggest the validity of the one-loop result. In $d=2$ and higher dimensions [10], numerical results indicated that possible corrections to the one-loop result were smaller than the two-loop estimates of Janssen [7].

Another important question is motivated by recent results on discrete models belonging to the Kardar-Parisi-Zhang (KPZ) class in $d=2$. The KPZ growth equation includes second-order linear and nonlinear terms which are more relevant than those in the VLDS equation [Eq. (1)] in the hydrodynamic limit [5,1]. Works on discrete KPZ models showed that the steady-state values of the moments of the height distribution,

$$W_n \equiv \langle \overline{(h-\overline{h})^n} \rangle, \tag{6}$$

obey power-counting, i.e., they scale as

$$W_n \sim L^{n\alpha} \tag{7}$$

(note that $W_2=\xi^2$). Moreover, estimates of the skewness

$$S \equiv \frac{W_3}{W_2^{3/2}} \tag{8}$$

and of the kurtosis

$$Q \equiv \frac{W_4}{W_2^2} - 3 \tag{9}$$

of the KPZ models indicated that the amplitude ratios of the moments W_n (such as S and Q) are universal [11–13]. It seems that no previous work has considered these questions in models belonging to the VLDS class, possibly due to the large times involved in their simulations (the dynamical exponent is nearly double that of the KPZ class). Besides the theoretical relevance of those questions, additional motivation for their analysis is the fact that the amplitude ratios can be measured with much higher accuracy than the scaling exponents and may eventually help one to infer the universality class of an experimental growth process.

There are a small number of discrete models belonging to the VLDS class in the continuum limit. The discrete model proposed by Das Sarma and Tamborenea (DT model) [14] is an example of a MBE-motivated model which falls in that class in $d=1$, although there is evidence that its class in $d=2$ is different [15,16]. On the other hand, the so-called conserved restricted-solid-on-solid (CRSOS) models, first proposed by Kim *et al.* [8], is expected to belong to the VLDS class in all dimensions. This was already proved analytically in $d=1$ [17–19]. In the CRSOS models, the difference in the heights of neighboring columns is always smaller than a certain value $\Delta H_{\max}$, similar to the RSOS model of Kim and Kosterlitz [20,21]. However, in the Kim-Kosterlitz model, if the aggregation at the column of incidence does not satisfy that condition, then the aggregation attempt is rejected (consequently, the model is in the KPZ class). On the other hand, in the CRSOS model, the incident particle migrates to the nearest column at which the height difference constraint is satisfied after aggregation. Thus, all deposition attempts are successful in the CRSOS model.

Here, we will study numerically a modified version of the CRSOS model in $d=1$ and $d=2$, with two different values of $\Delta H_{\max}$, the DT model in $d=1$, simulated with noise-reduction methods, and a competitive model involving CRSOS and random deposition in $d=1$. All these models belong to the VLDS class. We will perform systematic extrapolations of effective (roughness and dynamical) exponents for the CRSOS model in $d=1$ and $d=2$. The asymptotic exponents in $d=1$ are clearly different from the one-loop DRG values and the sign of the deviations are in qualitative agreement with Janssen's results [7]. In $d=2$, possible corrections in the exponent α are smaller than the two-loop corrections calculated in that work, confirming other authors' conclusions. It will also be shown that the moments of the heights distribution obey power-counting [Eq. (7)] in $d=1$ and $d=2$, similarly to KPZ, and that the skewness and the kurtosis for different versions of the CRSOS model (different $\Delta H_{\max}$) and for the competitive model have nearly the same values. These estimates differ from those of the DT model in $d=1$, but universality of amplitude ratios in the VLDS class cannot be discarded due to the typical long crossovers of the DT model.

The rest of this paper is organized as follows. In Sec. II, we present the stochastic rules of the CRSOS and DT models and give information on the simulation procedure. In Sec. III, we calculate the scaling exponents of the VLDS class in one-dimensional substrates. In Sec. IV, we calculate the scaling exponents in two-dimensional substrates. In Sec. V, we compare the asymptotic amplitude ratios of all models in $d=1$ and $d=2$. In Sec. VI, we summarize our results and present our conclusions.

II. MODELS AND SIMULATION PROCEDURE

The rules for choosing the aggregation point in our version of the CRSOS model are slightly different from the original ones. The present version was introduced in Ref. [22] as a model for amorphous carbon-nitrogen film growth, but only small lattices were analyzed there and, consequently, reliable estimates of scaling exponents were not obtained.

At any time, all pairs of neighboring columns are restricted to obey the condition $\Delta h \leqslant \Delta H_{\max}$, where Δh is the difference in the columns' heights and $\Delta H_{\max}$ is fixed. The deposition attempt begins with the random choice of one substrate column i. If the above condition is satisfied after aggregation of a new particle at the top of column i, then the aggregation takes place at that position. Otherwise, a nearest-neighbor column is randomly chosen (independently of its height) and the same test is performed. This process is continued until a column is chosen in which the new particle can be permanently deposited. Here, the cases $\Delta H_{\max}=1$ and $\Delta H_{\max}=2$ will be analyzed.

In the original version of the CRSOS model [8], the aggregation takes place at the nearest column in which the condition on height differences is satisfied, but in our version the incident particle performs a random walk along the substrate direction(s) while it searches for the aggregation point. The original model was proved to belong to the VLDS class in $d=1$ by different methods [17–19] and the coefficients of the VLDS equation were explicitly calculated for $\Delta H_{\max}=1$ [18,19]. Since our version does not change any symmetry of the original CRSOS model, it is also expected to be in that class. Notice, for instance, that there is no upward or downward current in our model due to the mechanism of random

walks for choosing the aggregation position (the random steps do not depend on the relative heights of the columns). It implies that the coefficient of the second-order height derivative of the growth equation [not shown in Eq. (1)] is exactly zero, the VLDS equation being the most plausible continuum description—see, e.g., the discussion in Ref. [23].

We will also study the DT model in $d=1$. In this model, the incident particle sticks at the top of the randomly chosen column i if it has one or two lateral neighbors at that position (a kink site or a valley, respectively). Otherwise, the neighboring columns (at the right and the left sides in $d=1$) are consulted. If the top position of only one of these columns is a kink site or a valley, then the incident particle aggregates at that point. If no neighboring column satisfies that condition, then the particle sticks at the top of column i. Finally, if both neighboring columns satisfy that condition, then one of them is randomly chosen.

In our simulations of the DT model, we used the noise reduction technique adopted in Ref. [24]. The noise reduction factor m is the number of attempts at a site for an actual aggregation process to occur [25,26]. Here, the value $m=10$ will be considered because it provided accurate estimates of scaling exponents in Ref. [24] from simulations in relatively small systems. On the other hand, the data for the original DT model present huge finite-size corrections (see, e.g., Ref. [27]).

In order to improve our discussion on the universality of amplitude ratios (Sec. V), we also simulated a competitive model in which the aggregation of the incident particle may follow two different rules: with probability p, the particle aggregates at the top of the column of incidence, such as in the random deposition (RD) model [1]; otherwise (probability $1-p$) it diffuses until finding a column i in which the condition $h_i - h_j \leq \Delta H_{\max}$ is satisfied for all nearest neighbors j after aggregation. Thus, the latter aggregation mechanism works for preserving the column heights' constraint of the CRSOS model. Extending previous conclusions on other competitive models [28,29], it is expected that this model is described asymptotically by the VLDS equation, similarly to the pure CRSOS model, but the coefficients ν_4 and λ_4 of the corresponding continuous equation [Eq. (1)] are expected to depend on p. In this paper, we will simulate the model with $p=0.25$ ($p=0$ is the pure CRSOS model).

The above models were simulated in $d=1$ in lattices of lengths ranging from $L=16$ to $L=1024$ for the CRSOS model with $\Delta H_{\max}=1$ and $\Delta H_{\max}=2$, from $L=16$ to $L=256$ for the DT model, and from $L=16$ to $L=512$ for the competitive model. For the CRSOS models, the number of realizations up to the steady state was typically 10^4 for the smallest lattices and nearly 500 for the largest lattices. The same applies to the DT model, but notice that the largest length in that case was just $L=256$. In $d=2$, the CRSOS model with $\Delta H_{\max}=1$ was simulated in lattices of lengths ranging from $L=16$ to $L=256$, and with $\Delta H_{\max}=2$ only until $L=128$. Whenever the number of realizations up to the steady state was smaller than 10^4, a larger number of realizations covering the growth and the crossover regions was generated. This allowed the calculation of crossover times (see below) with good accuracy in $d=1$.

The calculation of the moments of the height distribution at the steady states, W_n [Eq. (6)], followed along the same lines described in Ref. [13]. In order to estimate dynamical exponents, we used a recently proposed method to calculate a characteristic time τ_0 which is proportional to the time of relaxation to the steady state [30]. For fixed L, after calculating the saturation width $\xi_{\text{sat}}(L)$, τ_0 is defined through

$$\xi(L,\tau_0) = k\xi_{\text{sat}}(L), \tag{10}$$

with a constant $k \lesssim 1$. From the Family-Vicsek relation [31], it is expected that [30]

$$\tau_0 \sim L^z. \tag{11}$$

Here, we estimated τ_0 with k ranging from $k=0.4$ to $k=0.7$. Since the exponent z is large, the characteristic times τ_0 increase very fast with L. Consequently, for large k, the accuracy of τ_0 is low in large lattices. On the other hand, for small k, the times τ_0 in small lattices are also very small (near $\tau_0=1$) and, consequently, there are effects of the initial flat substrate. This is the reason why we chose a restricted range of k to analyze our data.

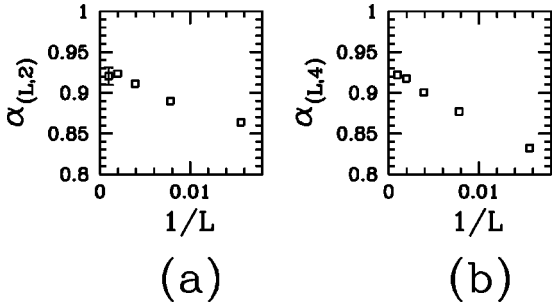

FIG. 1. Effective roughness exponents (a) $\alpha_{(L,2)}$ and (b) $\alpha_{(L,4)}$ versus inverse lattice length for the $(1+1)$-dimensional CRSOS model with $\Delta H_{\max}=1$. Error bars are shown only when they are larger than the size of the data points.

III. SCALING EXPONENTS IN ONE-DIMENSIONAL SUBSTRATES

In order to estimate the roughness exponent from the interface width ξ, the first step is to calculate the effective exponents

$$\alpha_{(L,i)} \equiv \frac{\ln[\xi_{\text{sat}}(L)/\xi_{\text{sat}}(L/i)]}{\ln i} \tag{12}$$

for fixed i. It is expected that $\alpha_{(L,i)} \to \alpha$ for any choice of i.

In Figs. 1(a) and 1(b), we show $\alpha_{(L,2)}$ and $\alpha_{(L,4)}$ versus $1/L$, respectively, for the CRSOS model with $\Delta H_{\max}=1$. The evolution of the data suggests that $\alpha_{(L,i)}$ converges to $0.91 \leq \alpha \leq 0.94$, accounting for the error bars and reasonable finite-size corrections.

The type of plot in Figs. 1(a) and 1(b) is suitable to fit the data to the scaling form

$$\alpha_{(L,i)} \approx \alpha + AL^{-\Delta}, \tag{13}$$

with A constant, if the correct variable $L^{-\Delta}$ is used in the abscissa [$\Delta=1$ was tested in Figs. 1(a) and 1(b)]. In its turn, Eq. (13) is a consequence of a scaling relation

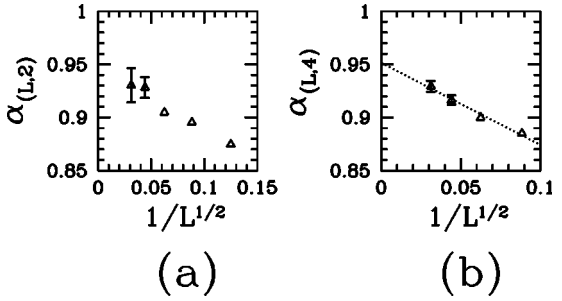

FIG. 2. Effective roughness exponents (a) $\alpha_{(L,2)}$ and (b) $\alpha_{(L,4)}$ versus $1/L^{1/2}$ for the (1+1)-dimensional CRSOS model with $\Delta H_{\max}=2$. Error bars are shown only when they are larger than the size of the data points.

$\xi_{\rm sat} \approx L^{\alpha}(a_0 + a_1 L^{-\Delta})$, with a_0 and a_1 constants, which includes a subdominant term in addition to the dominant one in Eq. (4). However, no variable of the form $L^{-\Delta}$ provided a reasonable linear fit in the range of lattice size analyzed there. Thus, $\Delta=1$ was used in Figs. 1(a) and 1(b) just to illustrate the L dependence of the effective exponents. On the other hand, estimating the asymptotic α is possible because there is no evidence of an upward curvature of those plots for large L.

The data for the CRSOS model with $\Delta H_{\max}=2$ were analyzed along the same lines. In Figs. 2(a) and 2(b), we show $\alpha_{(L,2)}$ and $\alpha_{(L,4)}$ versus $1/L^{1/2}$, respectively. The variable in the abscissa of Figs. 2(a) and 2(b) was chosen to provide a good linear fit of the $\alpha_{(L,4)}$ data—see the dotted line in Fig. 2(b). These results suggest stronger finite-size corrections for $\alpha_{(L,i)}$ when compared to the model with $\Delta H_{\max}=1$. The corresponding asymptotic estimates are in the range $0.92 \leqslant \alpha \leqslant 0.97$, also accounting for the error bars. However, since these error bars are larger than those for $\Delta H_{\max}=1$, it is possible that the true asymptotic regime was not attained yet and that the true leading corrections are different. Anyway, those results still suggest that $\alpha<1$ in the $L\to\infty$ limit.

Alternatively, we will analyze our data assuming the presence of a constant term as the subleading correction to the scaling of $\xi^2_{\rm sat}$,

$$\xi^2_{\rm sat} = \xi^2_I + AL^{2\alpha} \tag{14}$$

[since $\alpha \sim 1$, it corresponds asymptotically to $\Delta \sim 2$ in Eq. (13)]. ξ_I is called intrinsic width and is frequently associated to large local slopes in discrete KPZ models [25,26,13]. Effective exponents $\alpha^{(I)}_L$ which cancel the contribution of ξ^2_I may be defined as

$$\alpha^{(I)}_L \equiv \frac{1}{2}\frac{\ln[\xi^2_{\rm sat}(2L) - \xi^2_{\rm sat}(L)]/[\xi^2_{\rm sat}(L) - \xi^2_{\rm sat}(L/2)]}{\ln 2}. \tag{15}$$

In Figs. 3(a) and 3(b), we show $\alpha^{(I)}_L$ versus $1/L$ for the CRSOS model with $\Delta H_{\max}=1$ and $\Delta H_{\max}=2$, respectively. Here, the variable $1/L$ in the abscissa was also not chosen to perform data extrapolation. The effective exponents vary within narrow ranges (0.89–0.94 for $\Delta H_{\max}=1$, 0.90–0.96 for $\Delta H_{\max}=2$), even including their error bars. Consequently, any variable in the form $L^{-\Delta}$ $(0.5 \leqslant \Delta \leqslant 2)$ in the abscissa would lead to nearly the same extrapolated value of α. The data for $\Delta H_{\max}=1$ are more accurate and suggest $0.90 \leqslant \alpha \leqslant 0.95$, which is consistent with the previous analysis. The results for $\Delta H_{\max}=2$ confirm the trend to $\alpha<1$, although the uncertainties are larger.

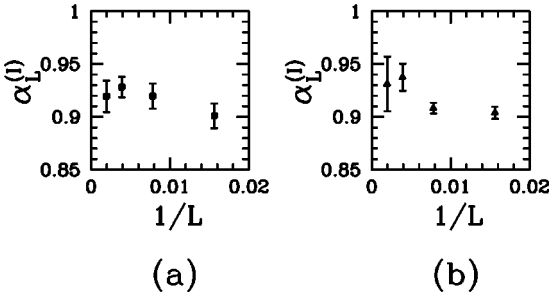

FIG. 3. Effective roughness exponents $\alpha^{(I)}_L$ (accounting for the intrinsic width) versus $1/L$ for (1+1)-dimensional CRSOS models with (a) $\Delta H_{\max}=1$ and (b) $\Delta H_{\max}=2$.

Assuming the power-counting property [Eq. (7)] of the moments of the width distribution (to be discussed in detail in Sec. V), we may also use higher moments to estimate α. The effective exponents obtained from W_3 have large fluctuations, but those obtained from W_4 behave similarly to the ones obtained from the interface width. They are defined as

$$\alpha^{(4)}_{(L,i)} \equiv \frac{\ln[W_{4,\rm sat}(L)/W_{4,\rm sat}(L/i)]}{\ln i}, \tag{16}$$

where $W_{4,\rm sat}(L)$ are the fourth moments calculated at the steady states.

In Figs. 4(a) and 4(b), we show $\alpha^{(4)}_{(L,2)}$ versus $1/L^{1/2}$ for the CRSOS models with $\Delta H_{\max}=1$ and $\Delta H_{\max}=2$, respectively. The variable in the abscissa of Figs. 4(a) and 4(b) was also chosen to illustrate the behavior of the data for large L and not to fit the data to a certain scaling form. The downward curvature of the plots for large L also suggests $\alpha<1$. The maximum and minimum reasonable limits that can be inferred from the evolution of the data for $\Delta H_{\max}=1$ give $0.92 \leqslant \alpha \leqslant 0.96$. The accuracy of the estimate for $\Delta H_{\max}=2$ is lower, as before.

The intersection of at least two of the above estimates for $\Delta H_{\max}=1$, obtained from the scaling of different quantities

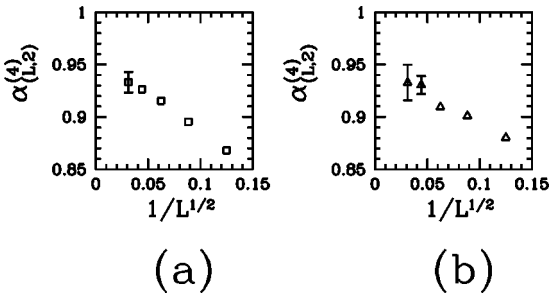

FIG. 4. Effective roughness exponents $\alpha^{(4)}_{(L,2)}$ (obtained from the fourth moment W_4) versus $1/L^{1/2}$ for (1+1)-dimensional CRSOS models with (a) $\Delta H_{\max}=1$ and (b) $\Delta H_{\max}=2$. Error bars are shown only when they are larger than the size of the data points.

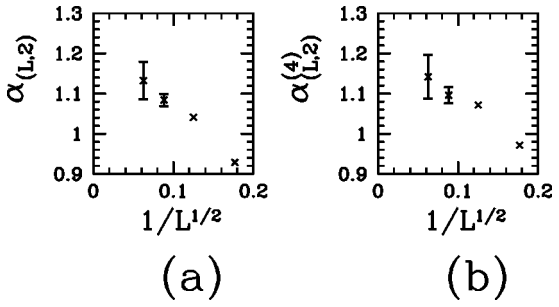

FIG. 5. Effective roughness exponents (a) $\alpha_{(L,2)}$ (obtained from the interface width) and (b) $\alpha^{(4)}_{(L,2)}$ (obtained from W_4) versus $1/L^{1/2}$ for the $(1+1)$-dimensional DT model. Error bars are shown only when they are larger than the size of the data points.

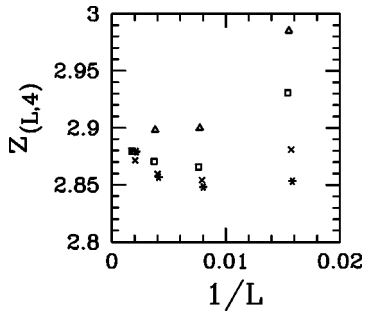

FIG. 6. Effective dynamical exponents $z_{(L,4)}$ versus $1/L$ for the $(1+1)$-dimensional CRSOS model with $\Delta H_{\max}=1$: $k=0.4$ (triangles), $k=0.5$ (squares), $k=0.6$ (crosses), $k=0.7$ (stars). Small horizontal shifts of the data points were used to avoid their superposition. Error bars (not shown) are smaller than $\Delta z=0.02$ (of this order for the largest L).

and assuming different forms of finite-size corrections, provides a final estimate $\alpha=0.94\pm0.02$. As will be discussed below, results for the DT model do not improve those obtained with the CRSOS model.

In Figs. 5(a) and 5(b), we show the effective exponents $\alpha_{(L,2)}$ and $\alpha^{(4)}_{(L,2)}$ for the noise-reduced DT model, also as a function of $1/L^{1/2}$. They are larger than $\alpha=1$ and systematically increase with L. However, from all previous theoretical work and the above numerical data for the CRSOS models, there is no reason to expect $\alpha>1$ in the VLDS class. Consequently, extrapolation of those data will not give reliable information for the discussion on the exponents of the VLDS theory in $1+1$ dimensions. Instead, it is expected that the effective exponents for the noise-reduced DT model [Figs. 5(a) and 5(b)] will eventually begin to decrease with L, possibly for much larger L. Such a decrease of $\alpha_{(L,2)}$ is actually observed in the original DT model (without noise reduction), in the same range of lattice lengths analyzed here [27]. Also recall that, as shown in Ref. [27], the data for the original DT model also present huge finite-size effects and cannot be used to obtain reliable estimates of VLDS exponents.

No improvement of the results in Figs. 5(a) and 5(b) is obtained by considering the contribution of the intrinsic width [Eqs. (14) and (15)].

There are two other points concerning our results for the DT model that deserve some comments. The first one is the comparison with the results of Punyindu and Das Sarma in Ref. [24], who obtained $\alpha\approx1$ with noise reduction in lattice lengths $L\lesssim60$. Our effective exponents for the smallest lattices ($16\leqslant L\leqslant64$) correspond to two data points at the left sides (larger $1/L$) of Figs. 5(a) and 5(b) and those exponents are also near $\alpha=1$. Consequently, our estimates are consistent with those of Ref. [24]. On the other hand, we conclude that the noise-reduction scheme works properly only in a special range of lattice lengths, since its application to larger lattices [$L=128$ and $L=256$ in Figs. 5(a) and 5(b)] led to effective exponents larger than 1, indicating much more complicated finite-size behavior.

The other important point is related to the large error bars, particularly for $L=256$. One of the reasons is certainly the relatively small number of realizations for the largest lengths (see Sec. II). However, the surfaces generated by the DT model in $d=1$ present grooves which may survive during long times. These structures largely increase the interface width of some realizations (see Ref. [32]) and, consequently, have a remarkable influence on the fluctuations of that quantity when averaged over various realizations. However, note that this instability is controlled in the DT model, i.e., the depths of the grooves do not diverge as time increases, contrary to other discretized growth models which show true instabilities when pillars or grooves are formed [32,33].

Now we turn to the calculation of the dynamical exponent.

Effective dynamical exponents are defined as

$$z_{(L,i)}=\frac{\ln[\tau_0(L)/\tau_0(L/i)]}{\ln i}, \tag{17}$$

so that $z_L\to z$ as $t\to\infty$. The error bars of τ_0 are larger than those of ξ and the uncertainties are enlarged in the calculation of effective exponents for small values of i [Eq. (17)], therefore we will work only with $i=4$.

In Fig. 6, we show $z_{(L,4)}$ versus $1/L$ for the CRSOS model with $\Delta H_{\max}=1$, with τ_0 calculated using four different values of k in Eq. (10) ($0.4\leqslant k\leqslant0.7$). The data for different k clearly converge to the same region, providing an asymptotic estimate $z=2.88\pm0.04$. This final estimate also accounts for the error bars (not shown in Fig. 6), which are near $\Delta z=0.02$ for the largest values of L. Again it is clear that the value $z=3$ of one-loop renormalization is excluded.

This conclusion is corroborated by the results for the CRSOS model with $\Delta H_{\max}=2$, although the accuracy of the data was poorer. In Fig. 7, we show $z_{(L,4)}$ versus $1/L$ for that model, with τ_0 also calculated using four different values of k in Eq. (10).

Our results for the noise-reduced DT model do not provide useful information on dynamical exponents, similar to the case of the roughness exponents.

IV. SCALING EXPONENTS IN TWO-DIMENSIONAL SUBSTRATES

In Figs. 8(a) and 8(b), we show $\alpha_{(L,2)}$ [Eq. (12)] and $\alpha^{(4)}_{(L,2)}$ [Eq. (16)] for the two-dimensional CRSOS model

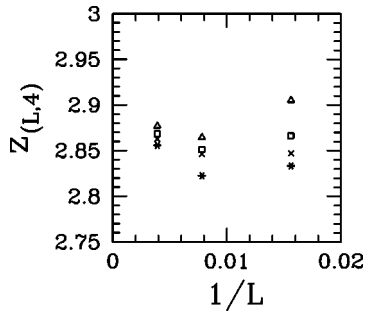

FIG. 7. Effective dynamical exponents $z_{(L,4)}$ versus $1/L$ for the (1+1)-dimensional CRSOS model with $\Delta H_{\max}=2$. Error bars (not shown) are smaller than $\Delta z=0.03$ (of this order for the largest L). Symbols correspond to the same values of k in Fig. 6.

with $\Delta H_{\max}=1$. Both linear fits give $\alpha=0.662$, which is very near the one-loop renormalization value $\alpha=\frac{2}{3}$ of the VLDS theory. Accounting for the error bars, which are particularly large for $L=256$, we are not able to determine whether $\alpha=\frac{2}{3}$ is exact or not. On the other hand, confirming other authors' results [10], any difference from that value is probably smaller than the two-loop correction of Janssen [7], which is $\Delta\alpha\approx 0.014$.

Similar to the one-dimensional case, the error bars of the data for the model with $\Delta H_{\max}=2$ are larger. Consequently, no discrepancy from the one-loop exponents could be detected too.

The characteristic times τ_0 for the model with $\Delta H_{\max}=1$ were obtained in lattices with $16\leqslant L\leqslant 128$, but their values for the smallest lattices ($L=16$ and $L=32$) are very small, sometimes below $\tau_0=1$ (one monolayer). For $L=256$, the accuracy of the interface widths data is not enough to provide reliable estimates of τ_0. Consequently, we were not able to calculate accurate dynamical exponents in the two-dimensional case.

V. UNIVERSALITY OF AMPLITUDE RATIOS

Evidence on the power-counting property of the moments W_n of the heights distribution of VLDS models was given in Sec. III by the estimates of α obtained from W_2 and

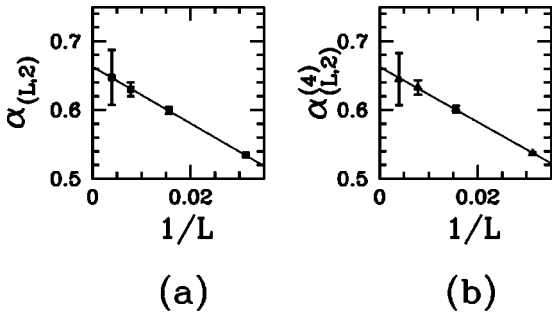

FIG. 8. Effective roughness exponents (a) $\alpha_{(L,2)}$ (obtained from the interface width) and (b) $\alpha^{(4)}_{(L,2)}$ (obtained from W_4) versus $1/L$ for the (2+1)-dimensional CRSOS model with $\Delta H_{\max}=1$. Error bars are shown only when they are larger than the size of the data points.

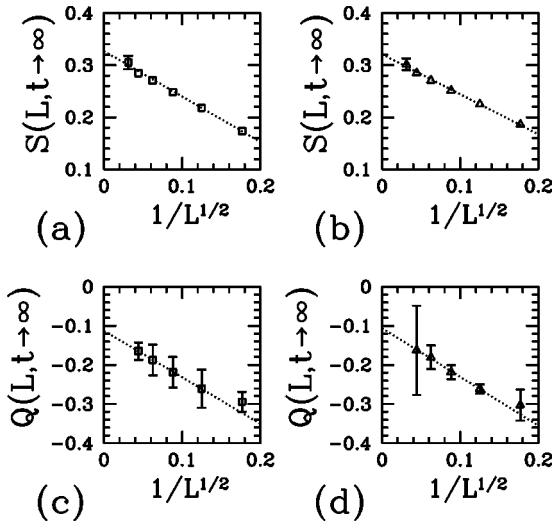

FIG. 9. Steady-state skewness for the (1+1)-dimensional CRSOS model with (a) $\Delta H_{\max}=1$ and (b) $\Delta H_{\max}=2$, and steady-state kurtosis for that model with (c) $\Delta H_{\max}=1$ and (d) $\Delta H_{\max}=2$, as functions of $1/L^{1/2}$. Dotted lines are least-squares fits of the data. Error bars are shown only when they are larger than the size of the data points.

W_4. Clearer evidence is given here by the finite asymptotic estimates of the skewness and the kurtosis at the steady states.

First we consider the models in 1+1 dimensions.

In Figs. 9(a) and 9(b), we show the steady-state skewness versus $1/L^{1/2}$ for the CRSOS models with $\Delta H_{\max}=1$ and $\Delta H_{\max}=2$, respectively. Except for the data for $L=1024$, which have relatively large error bars, all points fall in almost perfect straight lines, which give the asymptotic value $S=0.32\pm 0.02$ for both models.

In Figs. 9(c) and 9(d), we show the steady-state kurtosis versus $1/L^{1/2}$ for the CRSOS models with $\Delta H_{\max}=1$ and $\Delta H_{\max}=2$, respectively. Only the data for $L\leqslant 512$ were shown because the error bars are much larger for $L=1024$, not giving additional information on the evolution of Q. Reasonable linear fits are obtained with the last four data points in each case. The asymptotic estimate is $Q=-0.11\pm 0.02$ for both models.

Our results for the competitive model (RD and CRSOS) introduced in Sec. II also suggest that those amplitude ratios are universal for VLDS models. In that case, there is no constraint on the difference of the heights of neighboring columns, but only a trend to suppress large height differences. The coefficients ν_4 and λ_4 in the corresponding continuous equation [Eq. (1)] are probably different from those in the pure model ($p=0$), as obtained in related competitive models [28,29]. In Figs. 10(a) and 10(b), we show, respectively, $S(L,t\to\infty)$ and $Q(L,t\to\infty)$ as a function of $1/L^{1/2}$ for the competitive model. The asymptotic estimates are $S=0.32\pm 0.02$ and $Q\approx -0.1$, which are near the previous estimates for the pure CRSOS model.

In Figs. 10(c) and 10(d), we show, respectively, $S(L,t\to\infty)$ and $Q(L,t\to\infty)$ as a function of $1/L^{1/2}$ for the noise-reduced DT model in $d=1$. There are several reasons for the large error bars of the kurtosis, particularly in the

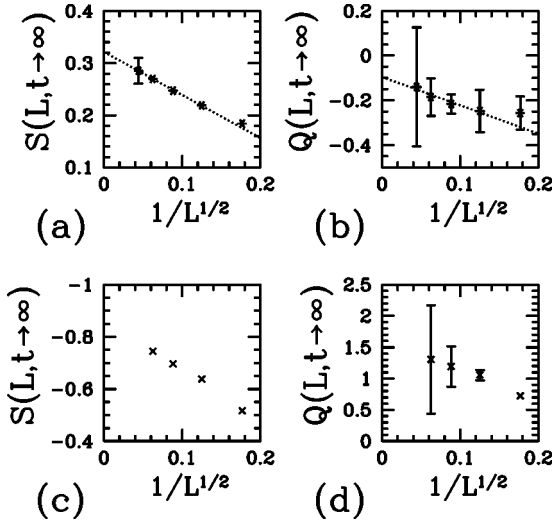

FIG. 10. (a),(b) Steady-state skewness and kurtosis, respectively, as a function of $1/L^{1/2}$, for the competitive model (CRSOS with $\Delta H_{\max}=1$ and RD); (c),(d) steady-state skewness and kurtosis, respectively, as a function of $1/L^{1/2}$, for the DT model. Dotted lines are least-squares fits of the data. Error bars are shown only when they are larger than the size of the data points.

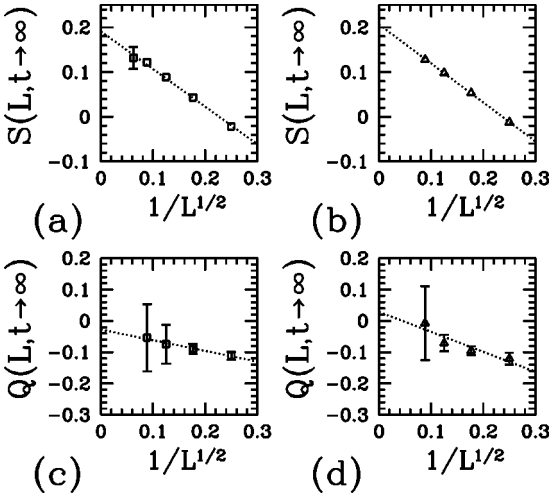

FIG. 11. Steady-state skewness for the $(2+1)$-dimensional CRSOS model with (a) $\Delta H_{\max}=1$ and (b) $\Delta H_{\max}=2$, and steady-state kurtosis for that model with (c) $\Delta H_{\max}=1$ and (d) $\Delta H_{\max}=2$, as functions of $1/L^{1/2}$. Dotted lines are least-squares fits of the data. Error bars are shown only when they are larger than the size of the data points.

largest lattices. First, as justified in Sec. III, fluctuations in the data for the DT model are typically large. Secondly, the relative fluctuations of the moments W_n [Eq. (6)] rapidly increase with the order n. Finally, while the size of the error bar of the kurtosis is the same as that of W_4/W_2^2, the relative error significantly increases when the constant 3 is subtracted [Eq. (9)]. The relatively large errors in Figs. 9(c) and 9(d) (CRSOS models) can also be explained along these lines.

The trends of the data for the DT model in Figs. 10(c) and 10(d) are completely different from those of the CRSOS models. We cannot exclude the possibility that the universality of the amplitude ratios might be a special feature of CRSOS models and some simple extensions, such as the above competitive model. However, the behavior of the scaling exponents of the DT model is also unusual, with no possible extrapolation to the expected region of the VLDS theory ($\alpha \leqslant 1, z \leqslant 3$), as discussed in Sec. III. Consequently, the present results for the DT model, although not confirming the universality of the amplitude ratios, are not enough to discard that hypothesis (the negative sign of the skewness is not a problem, since its sign changes with λ_4—see the related discussion in Ref. [13]).

Now we turn to the CRSOS models in $2+1$ dimensions.

In Figs. 11(a) and 11(b), we show the steady-state skewness versus $1/L^{1/2}$ for the CRSOS models with $\Delta H_{\max}=1$ and $\Delta H_{\max}=2$, respectively. The asymptotic estimates are $S=0.19\pm0.02$ and $S=0.20\pm0.02$, which also suggest the universality of this quantity. In Figs. 11(c) and 11(d), we show the steady-state kurtosis versus $1/L^{1/2}$ for the CRSOS models with $\Delta H_{\max}=1$ and $\Delta H_{\max}=2$, respectively. The asymptotic value $Q=0$, which is the Gaussian value, is consistent with the error bars. Thus, in $2+1$ dimensions, we also obtain evidence of universality of the amplitude ratios for CRSOS models, which suggests this possibility for the whole VLDS class.

VI. SUMMARY AND CONCLUSION

We studied numerically discrete growth models which belong to the VLDS class in $1+1$ and $2+1$ dimensions. Scaling exponents and steady-state values of the skewness and the kurtosis, which characterize the height distribution, were determined for those models.

Results for the CRSOS model with $\Delta H_{\max}=1$ gave the roughness exponent $\alpha=0.94\pm0.02$ and the dynamical exponent $z=2.88\pm0.04$ in $d=1$. These estimates confirm the proposal of Janssen [7] that the exponents of the VLDS theory obtained from one-loop renormalization ($\alpha=1$ and $z=3$) are not exact. The corrections from two-loop calculations give $\alpha\approx0.97$ and $z=2.94$, but they are obtained from expansions in $4-d$, which are not expected to provide accurate results for small d. On the other hand, the negative sign of the correction to one-loop results is consistent with our findings. In $d=2$, our results are not able to exclude the one-loop values, confirming other authors' conclusions [10].

The estimates of the steady-state skewness and kurtosis of the CRSOS models with $\Delta H_{\max}=1$ and $\Delta H_{\max}=2$ and of the competitive model (RD versus CRSOS with $\Delta H_{\max}=1$) suggest that those amplitude ratios are universal in the VLDS class. However, for the DT model in $d=1$, which belongs to the same class, those quantities are very different from the suggested universal values. One possible reason for this discrepancy is the slow convergence of the DT data to the VLDS behavior. The hypothesis of a slow crossover is supported by the fact that the estimates of α for the DT model are significantly larger than the values predicted theoretically and confirmed numerically ($\alpha \leqslant 1$ in $d=1$). Another possibil-

ity is that both CRSOS models and the competitive model have continuum representations with suitable combinations of coefficients which lead to the same forms of the heights distributions.

We believe that the results of this work will motivate further studies, numerical and analytical, of the VLDS equation and related discrete models. The estimates of scaling exponents in $d=1$ and the apparent universality of amplitude ratios are some of the results that may eventually help one to validate approximations in analytical works. On the other hand, numerical solutions of the VLDS equation or simulations of new discrete models in this class would be relevant to broaden the present discussion.

ACKNOWLEDGMENTS

The author acknowledges the useful suggestions of Professor H. K. Janssen and Professor S. Das Sarma. This work was partially supported by CNPq and FAPERJ (Brazilian agencies).

[1] A.-L. Barabási and H. E. Stanley, *Fractal Concepts in Surface Growth* (Cambridge University Press, New York, 1995).
[2] J. Krug, Adv. Phys. **46**, 139 (1997).
[3] J. Villain, J. Phys. I **1**, 19 (1991).
[4] Z.-W. Lai and S. Das Sarma, Phys. Rev. Lett. **66**, 2348 (1991).
[5] M. Kardar, G. Parisi, and Y.-C. Zhang, Phys. Rev. Lett. **56**, 889 (1986).
[6] E. Katzav, Phys. Rev. E **65**, 032103 (2002).
[7] H. K. Janssen, Phys. Rev. Lett. **78**, 1082 (1997).
[8] Y. Kim, D. K. Park, and J. M. Kim, J. Phys. A **78**, L533 (1994).
[9] Y. Kim, and J.-M. Kim, Phys. Rev. E **55**, 3977 (1997).
[10] S. H. Yook, J. M. Kim, and Y. Kim, Phys. Rev. E **56**, 4085 (1997).
[11] C.-S. Chin and M. den Nijs, Phys. Rev. E **59**, 2633 (1999).
[12] E. Marinari, A. Pagnani, and G. Parisi, J. Phys. A **33**, 8181 (2000).
[13] F. D. A. Aarão Reis, Phys. Rev. E **69**, 021610 (2004).
[14] S. Das Sarma and P. Tamborenea, Phys. Rev. Lett. **66**, 325 (1991).
[15] S. Das Sarma, P. P. Chatraphorn, and Z. Toroczkai, Phys. Rev. E **65**, 036144 (2002).
[16] A. Chame and F. D. A. Aarão Reis, Surf. Sci. **553**, 145 (2004).
[17] Z.-F. Huang and B.-L. Gu, Phys. Rev. E **57**, 4480 (1998).
[18] S.-C. Park, D. Kim, and J.-M. Park, Phys. Rev. E **65**, 015102 (2002).
[19] S.-C. Park, J.-M. Park, and D. Kim, Phys. Rev. E **65**, 036108 (2002).
[20] J. M. Kim and J. M. Kosterlitz, Phys. Rev. Lett. **62**, 2289 (1989).
[21] J. M. Kim, J. M. Kosterlitz, and T. Ala-Nissila, J. Phys. A **24**, 5569 (1991).
[22] F. D. A. Aarão Reis and D. F. Franceschini, Phys. Rev. E **61**, 3417 (2000).
[23] W. E. Hagston and H. Ketterl, Phys. Rev. E **59**, 2699 (1999).
[24] P. Punyindu and S. Das Sarma, Phys. Rev. E **57**, R4863 (1998).
[25] D. E. Wolf and J. Kertész, Europhys. Lett. **4**, 651 (1987).
[26] J. Kertész and D. E. Wolf, J. Phys. A **21**, 747 (1988).
[27] B. S. Costa, J. A. R. Euzébio, and F. D. A. Aarão Reis, Physica A **328**, 193 (2003).
[28] C. M. Horowitz and E. Albano, J. Phys. A **34**, 357 (2001).
[29] C. M. Horowitz, R. A. Monetti, and E. V. Albano, Phys. Rev. E **63**, 066132 (2001).
[30] F. D. A. Aarão Reis, Physica A **316**, 250 (2002).
[31] F. Family and T. Vicsek, J. Phys. A **18**, L75 (1985).
[32] C. Dasgupta, J. M. Kim, M. Dutta, and S. Das Sarma, Phys. Rev. E **55**, 2235 (1997).
[33] C. Dasgupta, S. Das Sarma, and J. M. Kim, Phys. Rev. E **54**, R4552 (1996).